Aperiodic diffraction grating based on the relationship between primes and zeros of the Riemann zeta function

© A.E. Madison,[1] D.A. Kozodaev,[2] A.N. Kazankov,[2] P.A. Madison,[1,3] V.A. Moshnikov[3]

[1]National Research University Higher School of Economics,
190121 St. Petersburg, Russia
[2]Active Photonics LLC,
124460 Zelenograd, Moscow, Russia
[3]St. Petersburg State Electrotechnical University „LETI",
197022 St. Petersburg, Russia
e-mail: alex_madison@mail.ru

The Riemann hypothesis is one of the most famous unsolved problems of modern science. One approach to proving the Riemann hypothesis is based on the assumption that the nontrivial zeros of the Riemann zeta function represent the spectrum of some self-adjoint operator. In this paper, we show that the duality with respect to the Fourier transform between the distribution of nontrivial zeros of the Riemann zeta function along the critical line, on the one hand, and the distribution of logarithms of prime numbers and powers of primes, on the other hand, can be used as a theoretical basis for creating new diffractive optical elements. In particular, we manufactured an aperiodic diffraction grating, the slits of which are ordered in accordance with the distribution of nontrivial zeros of the Riemann zeta function. Atomic force microscopy lithography was used for nanopatterning. The resulting diffraction pattern shows the presence of discrete diffraction maxima at the logarithms of primes and prime powers, which is the direct experimental visualization of the Hilbert−Polya conjecture.

Keywords: diffraction grating, atomic force microscopy lithography, Riemann zeta function, prime numbers.

DOI: 10.61011/JTF.2024.04.57538.285-23

Introduction

The Riemann hypothesis is one of the most complex unsolved problems of modern science [1–6]. One possible approach to proving the Riemann hypothesis relies on the Hilbert−Pólya conjecture that the non-trivial zeros of the Riemann zeta function may be interpreted by means of spectral theory [7,8]. Having analyzed the results of calculations performed by Odlyzko [9], Dyson noted that the distribution of zeros of the Riemann ξ-function may be regarded as a one-dimensional quasicrystal [10]. Specifically, he pointed out that „they constitute a distribution of point masses on a straight line, and their Fourier transform is likewise a distribution of point masses, one at each of the logarithms of ordinary prime numbers and prime-power numbers." More precisely, the resulting Fourier transform also contains, in addition to a discrete component, a continuous background component [11]. However, we may still regard both distributions as dual with respect to the Fourier cosine transform. The first distribution is an aperiodic sequence of Dirac δ-functions that reproduces, with a certain scale factor, the distribution of zeros of the Riemann ξ-function along the critical line. The second distribution is an aperiodic sequence of δ-functions that reproduces the sequence of prime numbers and powers of primes in a logarithmic scale.

If the first set of δ-functions corresponds to the positions of harmonic oscillators, its Fourier transform specifies the conditions of constructive interference of waves. The mathematical relations between such mutually dual discrete distributions may serve as a basis for construction of future diffractive optical elements. Specifically, a hypothetical Riemann interferometer consisting of an array of semitransparent mirrors placed at positions related to the logarithms of square-free integers was discussed in [8]. It was assumed that such a system of mirrors would provide an opportunity to visualize zeros of the Riemann ξ-function. However, we found no literature data on the construction of actual working instruments of this kind.

In the present study, we report on the fabrication of an aperiodic diffraction grating with alternating transparent and non-transparent sections. The fabricated structure differs from a common periodic grating in that its slits are ordered in accordance with the values of imaginary parts of non-trivial zeros of the Riemann zeta function (with a certain predetermined scale factor). Atomic force lithography was used for nanoprofiling. The obtained experimental diffraction patterns provided evidence of intense coherent scattering with a large number of well-resolved maxima

(even at large angles close to $90°$). As expected, the measured diffraction angles corresponded to logarithms of prime numbers and powers of primes. However, since the overall number of slits in fabricated gratings was relatively low, an exact correspondence was found only for the first maxima at the center of the diffraction pattern.

The conditions of constructive interference are normally formulated in the following way: the amplitudes of waves are summed if these waves arrive in phase relative to each other or, equivalently, if the difference in optical path for interfering beams from two neighboring slits to a point of interest on the screen is equal to an integer number of wavelengths [12–14]. In the present case, this universally accepted formulation is inapplicable. Our results demonstrate clearly that constructive interference from an aperiodic system of slits may be observed even if waves from any pair of neighboring slits arrive out of phase. The key requirement is the presence of a considerable discrete component in the Fourier transform of the corresponding aperiodic sequence of δ-functions.

The successful fabrication of an aperiodic diffraction grating based on the „hidden" order in the distribution of zeros of the Riemann ξ-function may stimulate further research into the construction of new optical instruments based on aperiodic deterministic structures [15–18], since these structures may exhibit features unattainable in periodic and stochastic systems. Experimental observations of the „spectrum" of non-trivial zeros of the zeta function may breathe a new life into systematic application of the spectral approach to various problems related to the Riemann hypothesis.

1. Theoretical relations

The Riemann hypothesis postulates that all non-trivial zeros of the Riemann ξ-function lie on the critical line (i.e., the real part of all non-trivial zeros is 1/2). At least at the present level of knowledge, the imaginary parts are distributed along the critical line in a fairly unpredictable way.

Let us imagine a system of narrow parallel slits with their positions reproducing accurately the positions of non-trivial zeros of the ξ-function on the critical line. If these slits are sufficiently narrow, the formed aperiodic diffraction grating may be regarded as a sequence of Dirac δ-functions. The corresponding diffraction pattern is characterized, in a first approximation, by a sum of complex exponentials over zeros of the Riemann ξ-function.

We have analyzed theoretically the series of this kind in [11] and found that partial sums of cosine series over zeros of the Riemann ξ-function are approximated fairly

accurately by the following expression:

$$S_N(t) = \sum_{k=-N}^{n} \cos(\gamma_k t) = 2\sum_{k=1}^{n} \cos(\gamma_k t)$$

$$\approx \left(2\pi\frac{N}{\gamma_N} + 1\right)\frac{\sin(\gamma_N t)}{\pi t} - \frac{\text{Si}(\gamma_N t)}{\pi t}$$

$$-\sum_{n=2}^{\infty}\frac{\Lambda(n)}{\sqrt{n}}\cdot\frac{\sin(\gamma_N(t\pm\ln n))}{\pi(t\pm\ln n)} + \exp(t/2) + \exp(-t/2).$$

Here, γ_k is the imaginary part of the kth zero. The first terms in this formula correspond to the central maximum, the last ones characterize the background, and the terms proportional to von Mangoldt function $\Lambda(n)$ correspond to diffracted beams.

Thus, the results reported in [11] allow us to formulate the following condition of coherent summing of waves (for a transmissive grating under normal beam incidence):

$$\frac{2\pi}{\lambda}a\sin\varphi = m\ln p.$$

Here, φ is the scattering angle, λ is the wavelength of incident radiation, a is the scale factor measured in μm (this implies that if γ_k is the imaginary part of the kth zero, the coordinate of position of the kth slit should be $a\gamma_k$), and p and p^m are prime numbers and powers of primes, respectively. In other words, we expect to see bright reflections on the screen at the positions of prime numbers and powers of primes in a logarithmic scale that is distorted slightly by the tangent of arcsine function. The relative brightness of reflections may be estimated by squaring the amplitudes of peaks in the Fourier spectrum ($I_{p,m} \propto A_{p,m}^2$), which are, in turn, specified by the corresponding values of von Mangoldt function $\Lambda(n)$:

$$A_{p,m} = \frac{\Lambda(n)}{\sqrt{n}} = p^{-m/2}\ln p.$$

2. Fabrication of an aperiodic grating and visualization of prime numbers

Atomic force lithography (AFM lithography) was used to form the needed pattern on the substrate surface. Different methods for nanoprofiling of the surface of samples via atomic force microscopy have been reviewed in [19–24].

Two major AFM lithography techniques are known: static lithography (engraving, scratching) and dynamic lithography (tapping). In the static case, the probe tip is in the contact mode. Lateral forces induced at the probe tip in the process of scratching bend and twist the cantilever, thus making the edges irregular and making it hard to reproduce accurately the shape and depth of scratches. A poorly controlled wrinkle relief may form when one tries to produce closely spaced parallel grooves. Another disadvantage of the static method consists in the fact that
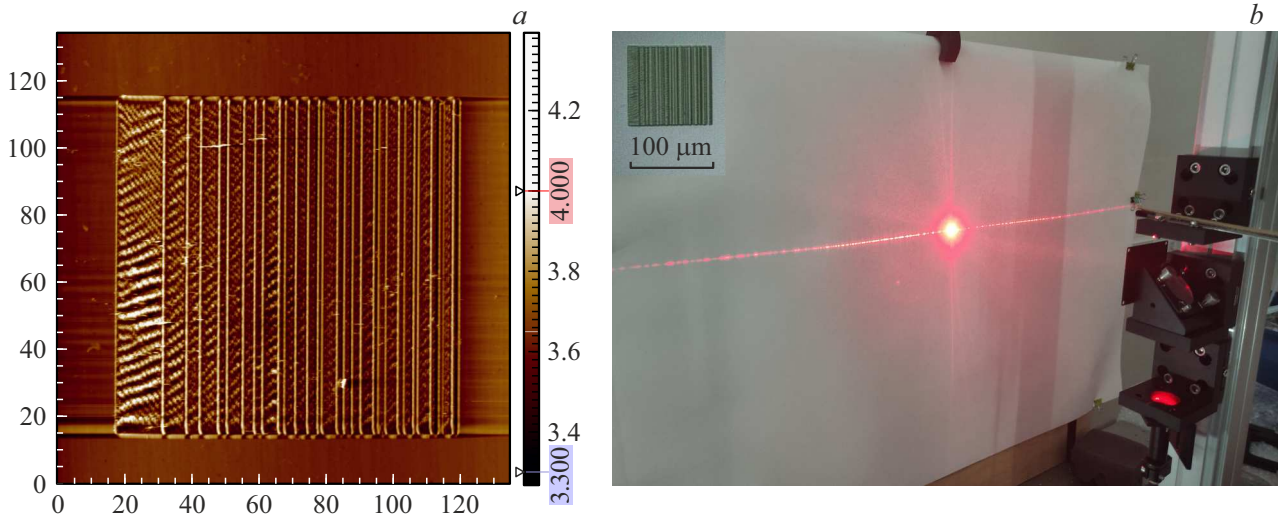
Figure 1. Aperiodic diffraction grating with its slits positioned in accordance with the distribution of zeros of the Riemann ξ-function: a — AFM image of a mini grating fabricated with a scale factor of $1.0\,\mu$m; b — experimental setup and diffraction pattern from the mini grating $100 \times 100\,\mu$m in size that was fabricated with a scale factor of $1.0\,\mu$m and features 29 slits. Its optical microphotographic image is shown in the inset in the upper left corner.

a probe wears out fast if large areas are to be scratched. Generally speaking, static AFM lithography is the easiest method, but also the least reproducible one.

In the case of dynamic nanolithography, the surface is modified by fast nanoindentation (point by point) by an oscillating probe in the tapping mode. This method provides fine reproducibility of patterning, and the obtained grooves are fairly uniform in shape and depth.

Note that the routine depth of a profile produced by dynamic lithography is on the order of several nanometers. Diffraction gratings designed for the visible spectral range normally require a much deeper surface relief. Structural elements with a characteristic size on the order of at least a hundred nanometers are needed. This is the primary reason why we chose the static method: as deep a relief as possible was preferable for our experiments. In addition, we performed multi-pass scratching with the probe shifted several times back and forth along the same line to deepen the grooves.

Thus, the problem consisted in forming the needed geometric pattern and transferring it to the substrate surface. We have written a program that performed the following functions: loading an array of zeros of the Riemann ξ-function from a resource file prepared in advance; calculation of slit positions for a given scale factor; determination of the boundaries of regions to be scratched; determination of the required probe motion trajectory; export of the obtained template as a vector image file. To scratch large areas between transparent „slits,“ we specified a complex meander-shaped trajectory with several closely spaced parallel lines and multiple passes along them.

An NTEGRA (LLC „NT-MDT“) atomic force microscope with an enlarged scanning area $(150 \times 150\,\mu$m) was used for surface modification. Several samples were prepared in order to test different materials, template parameter (area of the active region, scale factor, slit width, and pitch and number of passes) variations, and engraving parameter variations [25]. The best results were obtained in experiments with polyethylene terephthalate (SIQINZONGWA PET) substrates and a DRPS-In probe with single crystal diamond tip for deep scratching. The results for two samples reported below appear to be fairly reliable and informative.

The first sample was fabricated with scale factor $a = 1.0\,\mu$m. The diffraction region was $100 \times 100\,\mu$m in size and contained just 29 slits. The AFM image of the obtained mini grating is shown in Fig. 1, a. The average groove depth was measured to be approximately $250-300$ nm. It can be seen that wrinkle nanostructures of an irregular shape are present at the bottom of scratched regions. Unscratched regions remained transparent and served as slits.

This mini grating was secured to a holder and examined at a specially constructed measurement stand. The experimental setup and the obtained diffraction pattern are presented in Fig. 1, b. The optical micrograph of the grating is shown in the small inset in the upper left corner. A diode laser operating at a wavelength of 633 nm was used as a radiation source. The laser beam was directed to a mirror via a fiber. The sample was mounted on an optical table with a micropositioning system in such a way that the mirror reflected the beam to the active region. The diffraction pattern was observed on a screen located at a distance of 30 cm from the grating.

Although the area of the active region is relatively small, it generates a sufficiently intense field around itself (even at large scattering angles close to $90°$). Despite the fact that the grating is asymmetric, the diffraction pattern is
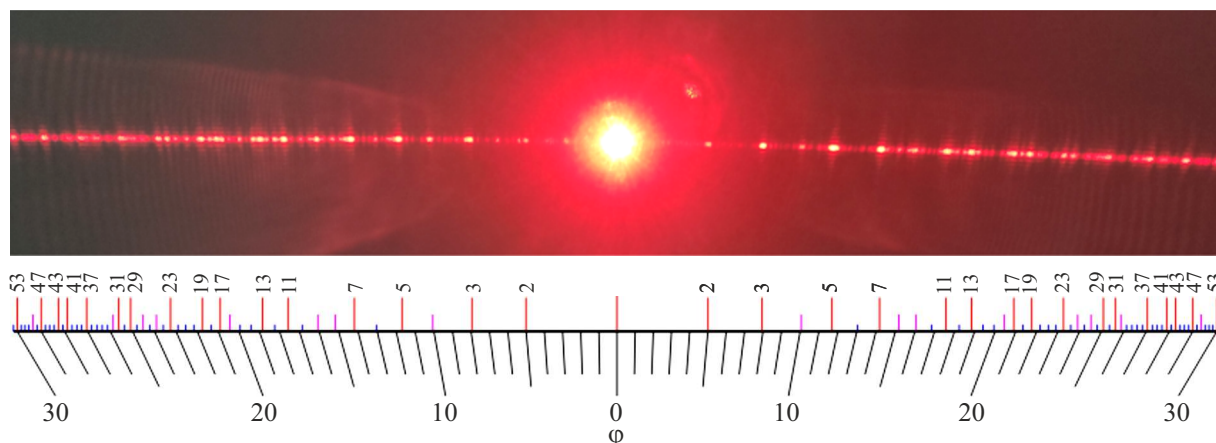
Figure 2. Interpretation of the diffraction pattern from the aperiodic grating with its slits positioned in accordance with the distribution of zeros of the Riemann ξ-function (the grating is $150 \times 150\,\mu$m in size, the scale factor is $0.8\,\mu$m, and 73 zeros are taken into account). Experimentally observed diffraction pattern (top); positions of prime numbers and powers of primes in a distorted logarithmic scale and the corresponding diffraction angles (bottom). Scale divisions correspond to natural numbers. Large scale marks denote prime numbers (strong reflections), medium-sized marks denote powers of primes (medium-intensity reflections), and the remaining natural numbers are designated with small marks (reflections are not observed).

symmetric. The central region of the diffraction pattern agrees closely with the theoretical prediction. Specifically, the first diffraction maxima emerge at angles of $\pm 4°$, which correspond to $\ln 2$ in the formula for constructive interference conditions.

A series of experiments with a Glan−Taylor prism introduced into the optical path were carried out in order to determine the influence of polarization of the incident beam on the overall shape of the diffraction pattern. Adjustment was performed in a standard way (with respect to the intensity maximum). No significant variations of the diffraction pattern were found in experiments with the incident beam polarized parallel and perpendicular to the slits.

The second sample was fabricated with scale factor $a = 0.8\,\mu$m within an area of $150 \times 150\,\mu$m. A total of 73 zeros of the Riemann ξ-function were taken into account in preparation of the template for fabrication. The number of slits was somewhat lower, since a single wide slit was formed instead of two overlapping ones if neighboring zeros of the Riemann ξ-function turned out to be positioned too close to each other. It was also taken into account that deep scratching could destroy fine protruding surface relief elements when the scale was decreased proportionally. In order to avoid this, we scaled down the corresponding technological process parameters of AFM lithography; as a result, the average surface relief modulation depth decreased to $80-100$ nm.

The diffraction pattern from the aperiodic grating fabricated with scale factor $a = 0.8\,\mu$m is shown in Fig. 2. Vertical marks on the (slightly distorted) logarithmic scale correspond to calculated positions of diffraction maxima. Large marks denote prime numbers (strong reflections), while medium-sized marks denote powers of primes

(medium-intensity reflections). The other natural numbers are denoted with small marks. No coherent summing of waves is observed for these numbers. Compression of a scattering object in the direct space leads to an inversely proportional stretching of the Fourier transform in the reciprocal space. In view of this, the first diffraction maxima for the grating fabricated with scale factor $0.8\,\mu$m emerge at angles of $\pm 5°$ (corresponding to $\ln 2$). Note also that the greater the number of zeros of the Riemann ξ-function taken into account in the process of fabrication of a grating is, the greater is the number of slits illuminated by a laser beam, and thus the greater is the nubmer of primes that may be resolved in the diffraction pattern.

Conclusion

The feasibility of fabrication of diffractive optical elements of a novel type (aperiodic diffraction gratings with slits ordered in accordance with the distribution of nontrivial zeros of the Riemann zeta function) was demonstrated. Atomic force nanolithography was used to prepare a series of samples differing in the substrate material, the active region size, the number of slits, the scale factor, the surface relief depth, and certain other minor parameters. Experimentally observed diffraction patterns produced by these aperiodic gratings visualize the duality between zeros of the Riemann zeta function and prime numbers.

It is too early to discuss the probable practical applications of these structures. However, their most noteworthy features are already evident: the number of reflections increases rapidly with scattering angle, and the scattering radiation intensity reaches significant levels at large angles (close to $90°$).

It is commonly assumed that a diffraction grating is a periodic structure that splits an input beam into several diffracted beams propagating in different directions. In the present case, the periodicity requirement is not necessary. The examined samples are examples of deterministic aperiodic structures.

Note also that mutual amplification of waves is assumed to occur when waves from neighboring sources arrive in phase relative to each other. The Bragg diffraction is an example of this. In the case of diffraction by deterministic aperiodic structures, the key requirement is the presence of a considerable discrete component in the Fourier transform of the corresponding aperiodic sequence of δ-functions.

Funding

Conflict of interest

The authors declare that they have no conflict of interest.

References

[1] B. Mazur, W. Stein. *Prime Numbers and the Riemann Hypothesis* (Cambridge University Press, 2015), DOI: 10.1017/CBO9781316182277

[2] H.M. Edwards. *Riemann's Zeta Function* (Dover Publications, Mineola, 2001), DOI: 10.1017/CBO9781316182277

[3] A.A. Coley. Phys. Scr., **92**, 093003 (2017). DOI: 10.1088/1402-4896/aa83c1

[4] A.A. Karatsuba, S.M. Voronin. *The Riemann Zeta-Function* (Walter de Gruyter, Berlin−NY., 1992), DOI: 10.1515/9783110886146

[5] A.A. Karatsuba. Russ. Math. Surv., **40**, 23 (1985). DOI: 10.1070/rm1985v040n05abeh003682

[6] M.A. Korolev. Kvant, **2020** (3), 10 (2020) (in Russian). DOI: 10.4213/kvant20200302

[7] M.V. Berry, J.P. Keating. SIAM Rev., **41**, 236 (1999). DOI:10.1137/S0036144598347497

[8] G. Sierra. Symmetry, **11**, 494 (2019). DOI: 10.3390/sym11040494

[9] A.M. Odlyzko. *Number Theory* (National Research Council, Washington, 1990), p. 35.

[10] F. Dyson. Not. Am. Math. Soc., **56**, 212 (2009). https://www.ams.org/notices/200902/rtx090200212p.pdf

[11] A.E. Madison, P.A. Madison, S.V. Kozyrev. Struct. Chem., **34**, 777 (2023). DOI: 10.1007/s11224-022-01906-2

[12] N.K. Pavlycheva. J. Opt. Technol., **89** (3), 142 (2022). DOI: 10.1364/JOT.89.000142

[13] N. Bonod, J. Neauport. Adv. Opt. Photon., **8**, 156 (2016). DOI: 10.1364/AOP.8.000156

[14] G. Zhou, Z.H. Lim, Y. Qi, F.S. Chau, G. Zhou. Int. J. Optomechatron., **15**, 61 (2021). DOI: 10.1080/15599612.2021.1892248

[15] L. Dal Negro (ed.) *Optics of Aperiodic Structures: Fundamentals and Device Applications* (Pan Stanford Publishing, Singapore, 2014), DOI: 10.1201/b15653

[16] E. Macia. Rep. Prog. Phys., **75**, 036502 (2012). DOI: 0.1088/0034-4885/75/3/036502

[17] L. Dal Negro, R. Wang, F.A. Pinheiro. Crystals, **6**, 161 (2011). DOI: 10.3390/cryst6120161

[18] A.S. Pirozhkov, E.N. Ragozin. Phys.-Uspekhi, **58**, 1095 (2015). DOI: 10.3367/UFNe.0185.201511d.1203

[19] R. Garcia, A.W. Knoll, E. Riedo. Nat. Nanotechnol., **9**, 577 (2014). DOI: 10.1038/nnano.2014.157

[20] S. Chang, Y. Geng, Y. Yan. Nat. Nanotechnol., **5**, 2 (2022). DOI: 10.1007/s41871-021-00115-5

[21] X. Xie, H. Chung, C. Sow, A. Wee. Mater. Sci. Eng. Rep., **54**, 1 (2022). DOI: 10.1016/j.mser.2006.10.001

[22] Y. He, Y. Yan, Y. Geng, E. Brousseau. Appl. Surf. Sci., **427 A**, 1076 (2018). DOI: 10.1016/j.apsusc.2017.08.134

[23] Y. Yan, S. Chang, T. Wang, Y. Geng. Polymers, **11**, 1590 (2019). DOI: 10.3390/polym11101590

[24] G. Liu, S.H. Petrosko, Z. Zheng, C.A. Mirkin. Chem. Rev., **120**, 6009 (2020). DOI: 10.1021/acs.chemrev.9b00725

[25] A.E. Madison, P.A. Madison, D.A. Kozodaev, A.N. Kazankov, V.A. Moshnikov. *HOLOEXPO 2023: 20-ya Mezhdunarodnaya konferentsiya po golografii i prikladnym opticheskim tekhnologiyam (Sochi, 12−15 sentyabrya): Tezisy dokladov* (Izd. S.-Peterb. Gos. Elektrotekh. Univ. „LETI," SPb., 2023), p. 69. ISBN 978-5-7629-3209-7 (in Russian).

Translated by D.Kondaurov